Asymptotic analysis of evaporating droplets

Nikos SAVVA[1,*], Alexey REDNIKOV[2], Pierre COLINET[2]

* Corresponding author: Tel.: +44(0)29 208 75116; Email: savvan@cf.ac.uk
1: School of Mathematics, Cardiff University, UK
2: TIPs - Fluid Physics Unit, Université Libre de Bruxelles, Belgium

Abstract We consider the evaporation dynamics of a two-dimensional, partially-wetting sessile droplet of a volatile liquid in its pure vapour, which is supported on a smooth horizontal superheated substrate. Assuming that the liquid properties remain unchanged, we utilise a one-sided lubrication-type model for the evolution of the droplet thickness, which accounts for the effects of evaporation, capillarity, slip and the kinetic resistance to evaporation. We follow an asymptotic approach, which yields a set of coupled evolution equations for the droplet radius and area, estimating analytically the evaporation-modified apparent angle when evaporation effects are weak. The validity of our matching procedure is verified by numerical experiments, obtaining also an estimate for the evaporation time.

Keywords: Drops, Evaporation, Wetting

1. Introduction

Droplet evaporation is a topic of active interest with applications in many different areas, ranging from microfluidic devices and the coating and cooling of surfaces to inkjet printing and DNA micro-arrays (see, for example, Erbil, 2012, and the references therein). In theoretical studies, droplet evaporation is typically considered in two different settings, namely the diffusion-limited evaporation into the ambient air (see, e.g., Deegan et al., 2000; Berteloot et al., 2008; Dunn et al., 2008; Eggers and Pismen, 2010) or the evaporation into a pure-vapour atmosphere (see, e.g., Anderson and Davis, 1995; Hocking, 1995; Ajaev, 2005).

In the former scenario, evaporation occurs due to the diffusion of vapour into the surrounding atmosphere, determining the vapour concentration as part of the solution. Conversely, when the droplet evaporates into its pure vapour, one typically invokes the one-sided model of evaporation developed by Burelbach et al. (1988). In this model, the dynamics of the liquid and evaporation are decoupled from those of the vapour and evaporation is determined by heat transfer through the liquid and non-equilibrium processes (kinetic resistance to evaporation) occurring at the free surface of the droplet.

In the present study, we assume the second scenario (pure-vapour atmosphere) using a minimal model which retains the main features of the evaporation process. We develop an asymptotic approach based on the disparity of scales between the size of the droplet and the size of a small region near the contact line, where the contact-line singularities are resolved. In this context, a common observation is that evaporation induces a change in the apparent contact angle above its equilibrium value determined by Young's relation (see, for example, Colinet and Rednikov, 2011; Janeček and Nikolayev, 2012, 2013; Rednikov and Colinet, 2013). The limit of weakly-modified apparent contact angles is investigated analytically, obtaining also an estimate of the evaporation time for a given initial volume.

2. Governing equation

Consider the dynamics of a two-dimensional partially-wetting sessile droplet of a volatile liq-

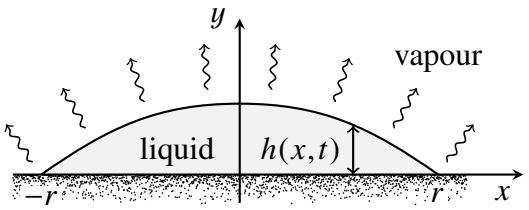

Figure 1: Sketch of the problem geometry.

uid in its pure vapour. The droplet is supported by a uniformly heated rigid horizontal surface which is kept at a temperature just above the vapour saturation temperature (see figure 1). Assuming that the liquid properties, namely the surface tension, density and viscosity all remain unchanged by temperature variations, we utilise the previously mentioned model by Burelbach et al. (1988).

Furthermore, assuming slow dynamics and that we have sufficiently small droplets so that we may neglect inertial and gravitational effects, respectively, in the end we obtain the following (appropriately non-dimensionalised) long-wave evolution equation for the droplet thickness, $h(x,t)$,

$$\partial_t h + \partial_x \left\{ h^2 (h+\lambda) \partial_x^3 h \right\} = -\frac{\mathscr{E}}{h+\mathscr{K}}, \quad (1)$$

which is valid for small contact angles, where λ corresponds to the slip length, $\mathscr{E}$ is the evaporation number and $\mathscr{K}$ is a non-equilibrium parameter, which compares the lengthscale over which kinetic effects of evaporation are appreciable with the droplet size. In this model we have neglected other effects, such as vapour recoil, thermocapillarity, the finite heat conductivity of the solid or heat loses to the vapour phase, which were partly included in other works (see, e.g., Anderson and Davis, 1995; Ajaev, 2005; Sodtke et al., 2008). These effects, however are not expected to affect qualitatively the phenomenology we wish to describe. Note also that the use of a slip model is not particularly restrictive apart from requiring that $\mathscr{K} \neq 0$. Using a different contact line model (for example a precursor film model - see, e.g. Ajaev, 2005; Colinet and Rednikov, 2011; Janeček and Nikolayev, 2013) is expected to exhibit qualitatively similar dynamics (see, e.g. Savva and Kalliadasis, 2011).

To solve (1) we impose a symmetry condition at the origin

$$\partial_x h|_{x=0} = 0, \quad (2)$$

whereas at the contact line, $x = r(t)$, we have

$$h|_{x=r} = 0 \quad \text{and} \quad \partial_x h|_{x=r} = -1, \quad (3a,b)$$

where the last condition fixes the contact angle to Young's equilibrium angle. Since we need to determine the location of the contact line as part of the solution, we also need to impose a condition of kinematic type. Looking into the asymptotics of (1) as $x \to r(t)$ yields

$$\dot{r} = \lambda\, h \partial_x^3 h\big|_{x=r} - \mathscr{E}\mathscr{K}^{-1}, \quad (4)$$

where the dot denotes differentiation with respect to t. Imposing other *ad hoc* conditions that prescribe, for example, a functional relation between the contact angle and the contact line speed does not offer any advantage on the treatment of the problem (Hocking, 1992).

Finally, if we define the (non-dimensional) cross-sectional area of the droplet as

$$a(t) = \int_{-r}^{+r} h \,\mathrm{d}x, \quad (5)$$

we can show that

$$\dot{a} = -\mathscr{E} \int_{-r}^{+r} \frac{1}{h+\mathscr{K}} \,\mathrm{d}x, \quad (6)$$

found simply by integrating (1) from $-r$ to $+r$.

3. Analysis

In this work, the problem is treated using matched asymptotics aiming to obtain a set of coupled equations for the evolution of $\dot{r}$ and $\dot{a}$. To do this, we note that all three parameters of the problem, λ, $\mathscr{E}$ and $\mathscr{K}$ are typically small. Moreover, previous results on the subject (see, e.g., Janeček and Nikolayev, 2012) suggest that evaporation effects become important in the vicinity of the contact line, as is the case with slip effects (see, e.g. Hocking, 1983). Hence to facilitate the analytical treatment of the problem via matched asymptotics,

we introduce the modified evaporation number, $E = \lambda^{-1}\mathscr{E}$ and the modified non-equilibrium parameter $K = \lambda^{-1}\mathscr{K}$, which allow us to use λ as the only small parameter of the problem.

3.1 Evolution of the droplet radius

The dynamics is expected to be slow so that $|\dot{r}| \ll 1$. Since, as previously mentioned, evaporation and slip effects are appreciable only within a region near the contact line, we may treat the contact line region separately from the bulk of the droplet. In the bulk, we neglect $O(\lambda)$ terms so that (1) becomes

$$\partial_t h + \partial_x \left\{ h^3 \partial_x^3 h \right\} = 0. \tag{7}$$

Using a quasistatic expansion in (7) of the form

$$h(x,t) = h_0(x,r,a) + \dot{r} h_1(x,r,a) + \ldots, \tag{8}$$

we collect powers of $\dot{r}$ to determine h_0 and h_1. At leading order we have $\partial_x^3 h_0 = 0$, to be solved subject to (2), (3a) and (5). This yields the parabolic profile

$$h_0(x,r,a) = \frac{\theta r}{2}\left(1 - \frac{x^2}{r^2}\right), \tag{9}$$

where θ can be identified as the apparent contact angle, given by

$$\theta = \frac{3a}{2r^2}. \tag{10}$$

At the next order, we obtain h_1 by solving

$$\partial_r h_0 + \partial_x \left\{ h_0^3 \partial_x^3 h_1 \right\} = 0, \tag{11}$$

where we have neglected the $O(\dot{a})$ terms in the bulk dynamics. Application of homogeneous conditions, $\partial_x h_1|_{x=0} = h_1|_{x=r} = \int_{-r}^{+r} h_1 \, \mathrm{d}x = 0$, allows us to deduce an exact solution for h_1. Nevertheless, in order to match with the dynamics near the contact line, it suffices to consider the behaviour of the slope as $x \to r$, namely $\partial_x h_1 \sim -\ln\left[\mathrm{e}^2(1-x/r)/2\right]/\theta^2$. Thus, using (8), we get

$$-\partial_x h \sim \theta + \frac{\dot{r}}{\theta^2} \ln\left[\frac{\mathrm{e}^2}{2}\left(1 - \frac{x}{r}\right)\right] \tag{12}$$

as $x \to r$.

Noting that in considering the flow in the bulk we have not utilised the contact angle condition (3b), we also need to look at the dynamics near the contact line. Based on (12) we anticipate the following asymptotic behaviour as we move from the contact line towards the bulk, or, equivalently, as $(r-x)/\lambda \to \infty$

$$-\partial_x h \sim \theta_m + \frac{\dot{r}}{\theta_m^2} \ln\left(\beta \frac{r-x}{\lambda}\right), \tag{13}$$

where θ_m is the macroscopic Young's angle modified by evaporation and β is a constant to be determined.

To investigate the behaviour near the contact line, we introduce the stretched variables

$$\phi = \frac{h}{\lambda} \quad \text{and} \quad \xi = \frac{r-x}{\lambda}, \tag{14}$$

which allow us to write (1) as

$$\dot{r}\partial_\xi \phi + \partial_\xi \left\{ \phi^2(\phi+1)\partial_\xi^3 \phi \right\} = -\frac{E}{\phi + K} \tag{15}$$

where we have retained $O(\lambda^0)$ terms only. Under this change of variables, (13), transforms to

$$\partial_\xi \phi \sim \theta_m + \frac{\dot{r}}{\theta_m^2} \ln \beta\xi \quad \text{as} \quad \xi \to \infty. \tag{16}$$

In the non-volatile case, $\theta_m = 1$ and $\beta = \mathrm{e}$ (see, e.g. Savva and Kalliadasis, 2009). Here we will only treat the case when θ_m is weakly modified by evaporation, taking $\theta_m = 1 + \alpha E$ with $\alpha E \ll 1$, where α is a constant to be determined. To proceed, we assume an expansion of the form

$$\phi = \xi + \tilde{\phi} + \ldots, \tag{17}$$

where $\xi \gg \tilde{\phi}$. It is easy to see that $\tilde{\phi}$ satisfies

$$\dot{r} + \partial_\xi \left\{ \xi^2 (\xi+1) \partial_\xi^3 \tilde{\phi} \right\} = -\frac{E}{\xi + K}. \tag{18}$$

To solve this boundary-value problem, we apply homogeneous conditions at $\xi = 0$

$$\tilde{\phi} = \partial_\xi \tilde{\phi} = 0, \tag{19}$$

with the asymptotics of $\tilde{\phi}$ as $\xi \to \infty$ given by

$$\partial_\xi \phi \sim \alpha E + \dot{r} \ln \beta\xi. \tag{20}$$

A careful consideration of (18) and its aforementioned conditions yields

$$\alpha = \int_0^\infty \frac{1}{\xi(\xi+1)} \ln\frac{K}{\xi+K}\, d\xi, \qquad (21)$$

$$\beta = \mathrm{e}, \qquad (22)$$

where we note that α can be evaluated analytically to get

$$\alpha = \mathrm{dilog}\, K + \frac{1}{2}\ln^2 K + \frac{\pi^2}{6}, \qquad (23)$$

where $\mathrm{dilog}\, K$ denotes the dilogarithm function. To conform with the requirement that $\alpha E \ll 1$, we find that if K is small, good agreement is expected if E is chosen so that

$$E \ll \frac{6}{2\pi + 3\ln^2 K}, \qquad (24)$$

whereas if K large, it suffices to choose

$$E \ll \frac{K}{1+\ln K}. \qquad (25)$$

This suggests that $1+\alpha E$ can be an acceptable approximation to θ_m for sufficiently large K, even when $E = O(1)$. When E and K do not conform with these requirements determining θ_m and β needs to be done numerically.

Figure 2 shows some representative computations comparing numerically determined values of θ_m (solid curves) and their weakly-modified form, $\theta_m = 1+\alpha E$ (dashed curves). We see that indeed excellent agreement is observed provided that E is sufficiently small and K sufficiently large. We also note that evaporation always enhances θ_m, but its effect is diminished as K becomes too large and/or E too small. These results are qualitatively consistent with those of Rednikov et al. (2009), who used a disjoining pressure model, the main difference being the presence of a weak singularity of θ_m in our model observed as $K \to 0$.

With these considerations, we have fully specified the behaviour of the dynamics in the vicinity of the contact line, (13), which is to be matched with (12). Following earlier works (e.g. Hocking, 1983; Savva and Kalliadasis, 2009), it turns out that we can match the cubes

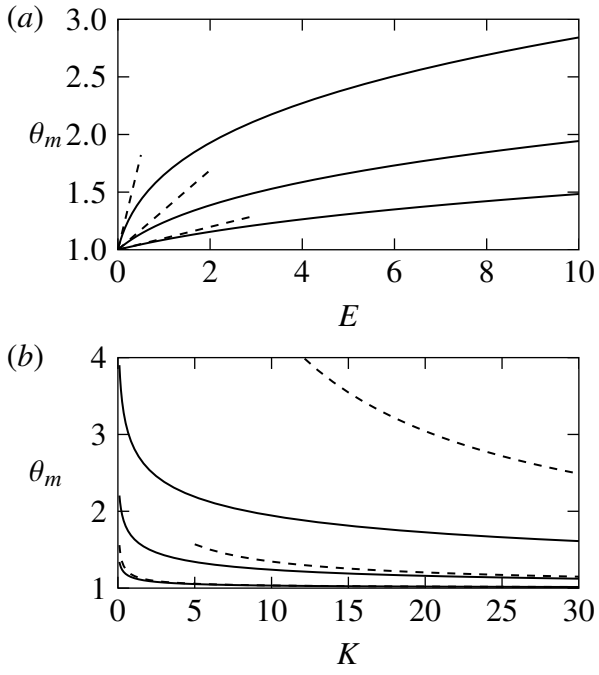

Figure 2: Dependence of θ_m on E and K comparing numerics (solid curves) with the asymptotic form, $\theta_m = 1+\alpha E$ (dashed curves). (a) Variation with E for various values of K; curves from top to bottom correspond to $K = 1$, 10 and 50, respectively. (b) Variation with K for various values of E; curves from top to bottom correspond to $E = 10$, 1 and 0.1, respectively.

of (12) and (13), thus allowing us to eliminate the r-dependent logarithmic terms to yield

$$\dot{r} = \frac{\theta^3 - \theta_m^3}{3\ln\dfrac{2r}{\mathrm{e}^2\lambda}}, \qquad (26)$$

which is valid for $\dot{r}$ up to $O(\ln\lambda^{-1})$.

3.2 Evolution of the droplet area

An estimate for the rate of change of the droplet area is found simply from (6) and using as an approximation to h the leading-order outer solution, h_0, given by (9). It is a matter of simple algebra to show that

$$\dot{a} = -\frac{4\lambda E}{\theta\sqrt{1+\eta}}\,\mathrm{arctanh}\left(\frac{1}{\sqrt{1+\eta}}\right), \qquad (27)$$

where $\eta = 2K\lambda/(r\theta)$. This is a leading-order calculation that neglects small contribu-

tions due to the $O(\dot{r})$ terms and due to the bending of the free surface near the contact line. When $\eta \ll 1$, i.e. when kinetic effects are small or for sufficiently large droplets, (27) becomes

$$\dot{a} = -\frac{2\lambda E}{\theta} \ln \frac{2r\theta}{K\lambda} + O(\eta) \qquad (28)$$

whereas when kinetic effects are significant so that $\eta \gg 1$ we have

$$\dot{a} = -\frac{2E\theta r}{K} + O\left(\eta^{-2}\right). \qquad (29)$$

It is important to note that when $\eta = O(1)$ there will not be a clear separation of lengthscales for our asymptotic analysis to be valid and naturally the applicability of (29) is questionable in this limit.

4. Results

From this analysis, we obtained (26) and (27), which constitute a coupled system of differential equations for the radius and area of the droplet. In this section we will compare the solutions to this system with solutions to the governing equation (1) and boundary conditions, (2) and (3) for a few representative cases, keeping λ fixed at 10^{-4} in all examples presented.

Figure 3 shows the result of a computation in a regime where θ_m is weakly-modified by evaporation, so that taking $\theta_m = 1 + \alpha E$ is an appropriate approximation. In figure 3*a* we show the evolution of the droplet area and volume and in figure 3*b* the evolution of the apparent contact angle when $E = 1$ and $K = 50$. We readily confirm the excellent agreement of the solution to the governing problem, (1)–(3), with that of the system of equations obtained from matching, (26) and (27). From these two plots we can identify four stages in the dynamics. Initially, there is a quick relaxation to the quasi-static dynamics - this stage is typically very brief. In the second stage, the motion is driven by the contact lines until the apparent contact angle θ relaxes to the macroscopic, evaporation-modified Young's angle, θ_m. In these two stages, we note that the area of the droplet does not change appreciably. In the third-stage, most of the area

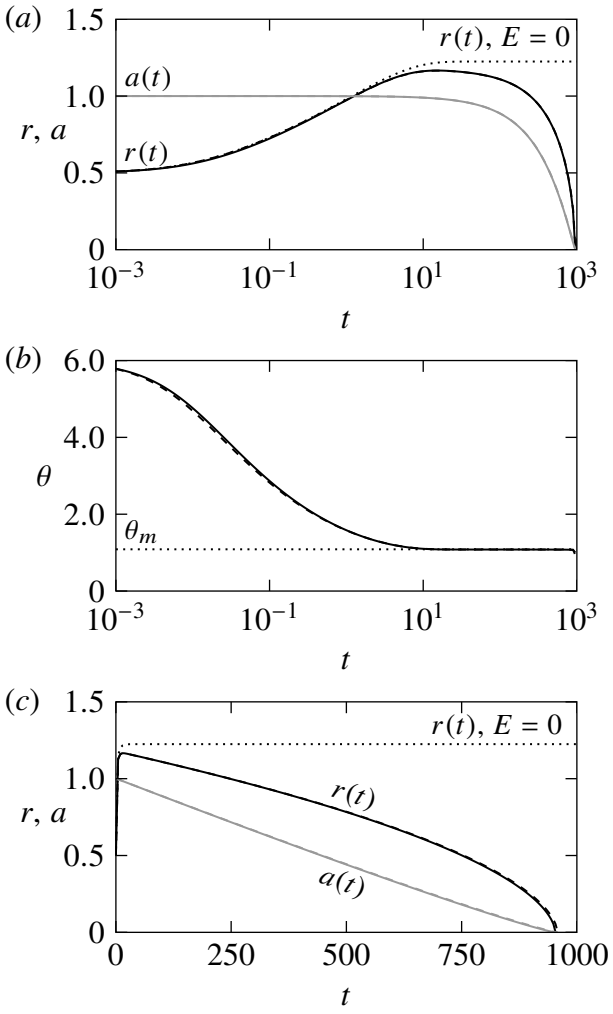

Figure 3: Verification of asymptotics in the weak-evaporation limit when $E = 1$, $K = 50$ and $\lambda = 10^{-4}$ with $r(0) = 0.5$ and $a(0) = 1$. The curves comparing the solutions obtained by matched asymptotics (dashed curves) with the full numerical solutions to (1) (solid curves) are nearly indistinguishable. (*a*) Evolution of the area (grey curves) and the radius (black curves); the dotted curve corresponds to the evolution of the radius in the non-volatile case. (*b*) Evolution of the apparent contact angle; the dotted line corresponds to the evaporation-modified macroscopic Young's angle. (*c*) As in (*a*), but for a linearly scaled t-axis.

of the droplet evaporates with $\theta \approx \theta_m$. In the final stage of evaporation, the droplet becomes too small to have a clear separation of lengthscales and our asymptotic analysis is, in principle, inapplicable. The evolution of $r(t)$ and $a(t)$

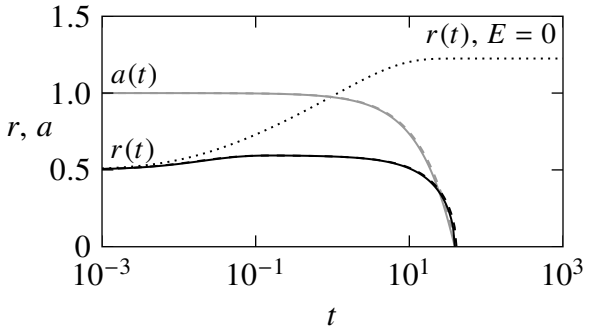

Figure 4: Evolution of the droplet radius and area in the strong-evaporation limit when $E = 50$, $K = 1$ and $\lambda = 10^{-4}$ with $r(0) = 0.5$ and $a(0) = 1$. The curve styles are as in figure 3*a*.

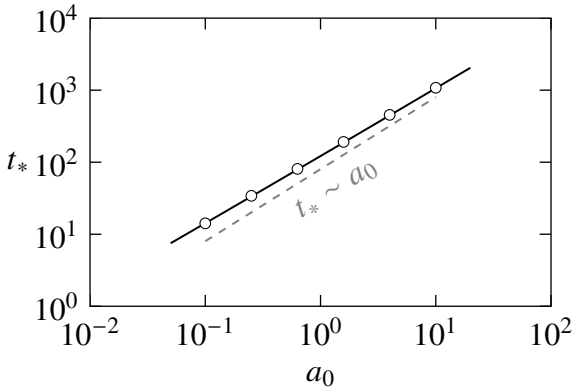

Figure 5: Evaporation time as a function of the initial droplet area when $E = 10$, $K = 10$ and $\lambda = 10^{-4}$. The solid curve corresponds to the theoretical prediction (31) and the circles to the numerics of the governing problem, (1)–(3); the dashed grey curve corresponds to the simple scaling $t_* \sim a_0$.

in the evaporation-dominated stages becomes more transparent when we use a linear scaling for the t-axis (see figure 3*c*).

The distinction and duration of these stages is strongly dependent on the parameters of the problem. For example, in the strong evaporation regime, the spreading phase may be too brief or we may even have contact line recession. An example where the contact line hardly spreads is given in figure 4 which is to be contrasted with the results of figure 3*a*, noting that in both cases we have used the same initial conditions. It is also worth mentioning that in order to preserve the excellent agreement between the solution to the governing equation and our asymptotic analysis shown in figure 4, we have computed θ_m numerically since our asymptotic result $\theta_m = 1 + \alpha E$ is no longer applicable.

From the preceding discussion, it is apparent that most of the evaporation takes place during the third stage for which we have $\theta \approx \theta_m$. In this stage, we may neglect the contact-line dynamics in (26) and consider only the evolution equation for $a(t)$. More specifically, consider (28) with (10) to get a differential equation in $a(t)$ only

$$\dot{a} = -\frac{2\lambda E}{\theta_m} \ln \frac{2\sqrt{3\theta_m a}}{K\lambda}. \tag{30}$$

This has an exact solution in terms of the exponential integral. Considering the asymptotics of the solution and using $a(0) = a_0$, we find that the time t_* required for the droplet to evaporate is given approximately by

$$t_* \approx \frac{a_0\theta_m}{\lambda E \ln \dfrac{12 a_0 \theta_m}{\mathrm{e} K^2 \lambda^2}}. \tag{31}$$

As it turns out, (31) is remarkably accurate despite the simplifying assumptions that lead to it. This is demonstrated in figure 5 where we compare the asymptotic result, (31), with the solutions to (1)–(3) with $E = K = 10$. For comparison, we have also included the scaling $t_* \sim a_0$, which can be obtained by simple scaling arguments, highlighting the importance of the logarithm in (31) in modulating the power law.

5. Concluding remarks

We have considered a simple model that is able to capture the combined evaporation and contact-line dynamics for two-dimensional droplets. The asymptotic analysis we performed allowed us to obtain a rather simple system of differential equations for the evolution of the droplet area and radius, valid for sufficiently large droplets and weak evaporation effects. For stronger evaporation effects the inner-region contact-line dynamics needs to be resolved numerically in order to obtain the macroscopic Young's angle modified by evaporation.

The solutions to the equations obtained by matching exhibit excellent agreement with the governing partial differential equation when considered in different settings. One can generalise the asymptotic analysis to treat more involved evaporation models by a careful extension of the arguments presented here. This is a subject of current investigation.

References

Ajaev, V.S., 2005. Spreading of thin volatile liquid droplets on uniformly heated surfaces. J. Fluid Mech. 528, 279–296.

Anderson, D.M., Davis, S.H., 1995. The spreading of volatile liquid droplets on heated surfaces. Phys. Fluids 7, 248–265.

Berteloot, G., Pham, C.T., Daerr, A., Lequeux, F., Limat, L., 2008. Evaporation-induced flow near a contact line: Consequences on coating and contact angle. Europhys. Lett. 83, 14003.

Burelbach, J.P., Bankoff, S.G., Davis, S.H., 1988. Nonlinear stability of evaporating/condensing liquid films. J. Fluid Mech. 195, 463–494.

Colinet, P., Rednikov, A., 2011. On integrable singularities and apparent contact angles within a classical paradigm. Eur. Phys. J. Special Topics 197, 89–113.

Deegan, R., Bakajin, O., Dupont, T., Huber, G., Nagel, S., Witten, T., 2000. Contact line deposits in an evaporating drop. Phys. Rev. E 62, 756–765.

Dunn, G., Wilson, S., Duffy, B., David, S., Sefiane, K., 2008. A mathematical model for the evaporation of a thin sessile liquid droplet: Comparison between experiment and theory. Colloids and Surf. A: Physicochem. Eng. Aspects 323, 50–55.

Eggers, J., Pismen, L.M., 2010. Nonlocal description of evaporating drops. Phys. Fluids 22, 112101.

Erbil, H.Y., 2012. Evaporation of pure liquid sessile and spherical suspended drops: A review. Adv. Colloid Interface Sci. 170, 67–86.

Hocking, L.M., 1983. The spreading of a thin drop by gravity and capillarity. Q. J. Mech. Appl. Math. 36, 55–69.

Hocking, L.M., 1992. Rival contact-angle models and the spreading of drops. J. Fluid Mech. 239, 671–781.

Hocking, L.M., 1995. On contact angles in evaporating liquids. Phys. Fluids 7, 2950–2955.

Janeček, V., Nikolayev, V., 2013. Apparent-contact-angle model at partial wetting and evaporation: Impact of surface forces. Phys. Rev. E 87, 012404.

Janeček, V., Nikolayev, V.S., 2012. Contact line singularity at partial wetting during evaporation driven by substrate heating. Europhys. Lett. 100, 14003.

Rednikov, A., Colinet, P., 2013. Singularity-free description of moving contact lines for volatile liquids. Phys. Rev. E 87, 010401.

Rednikov, A.Y., Rossomme, S., Colinet, P., 2009. Steady microstructure of a contact line for a liquid on a heated surface overlaid with its pure vapor: Parametric study for a classical model. Multiphase Sci. and Technol. 21, 213–248.

Savva, N., Kalliadasis, S., 2009. Two-dimensional droplet spreading over topographical substrates. Phys. Fluids 21, 092102.

Savva, N., Kalliadasis, S., 2011. Dynamics of moving contact lines: A comparison between slip and precursor film models. Europhys. Lett. 94, 64004.

Sodtke, C., Ajaev, V.S., Stephan, P., 2008. Dynamics of volatile liquid droplets on heated surfaces: theory versus experiment. J. Fluid Mech. 610, 343–362.